Journal of Advances in Mathematics and Computer Science

25(6): 1-20, 2017; Article no.JAMCS.38677
ISSN: 2456-9968
(Past name: British Journal of Mathematics & Computer Science, Past ISSN: 2231-0851)

DRBEM Sensitivity Analysis and Shape Optimization of Rotating Magneto-Thermo-Viscoelastic FGA Structures Using Golden-Section Search Algorithm Based on Uniform Bicubic B-Splines

Mohamed Abdelsabour Fahmy[1,2*]

[1]Faculty of Computers and Informatics, Suez Canal University, New Campus, 4.5 Km, Ring Road, El Salam District, 41522 Ismailia, Egypt.
[2]Jamoum University College, Umm Al-Qura University, Alshohdaa 25371, Jamoum, Makkah, Saudi Arabia.

Author's contribution

The sole author designed, analyzed and interpreted and prepared the manuscript.

Article Information

DOI: 10.9734/JAMCS/2017/38677
Editor(s):
(1) Octav Olteanu, Professor, Department of Mathematics-Informatics, University Politehnica of Bucharest, Bucharest, Romania.
Reviewers:
(1) Alok Kumar Pandey, Roorkee Institute of Technology, India.
(2) A. A. Opanuga, Covenant University, Nigeria.
Complete Peer review History: http://www.sciencedomain.org/review-history/22562

Original Research Article

Received: 7th December 2017
Accepted: 29th December 2017
Published: 2nd January 2018

Abstract

Aims: A practicalshape optimization technique is developed, using thedual reciprocity boundary element method (DRBEM) with the golden-section search algorithm based on uniform bicubic B-splines, for rotating magneto-thermo-viscoelastic functionally graded anisotropic (FGA) structures subjected to a moving heat source in the context of the Green and Naghdi theory of type III.
Study Design: Original Research Paper.
Place and Duration of Study: Jamoum University College, Mathematics Department, between July 2016 and August 2017.
Methodology: An implicit-implicit staggered algorithm was proposed for use with the DRBEM to obtain the final DRBEM coupled linear system of equations for displacements and temperature that describe the magneto-thermo-viscoelastic structural analysis problem. An implicit differentiation of the discretized dual reciprocity boundary integral equation with respect to design variables is used to calculate shape displacement sensitivities of anisotropic materials with very high accuracy. This method allows the coupling between optimization technique and a dual reciprocity boundary element method. The feasible direction method was developed and implemented for use with the one-dimensional golden-section search

**Corresponding author: E-mail: mohamed_fahmy@ci.suez.edu.eg;*

technique based on uniform bicubic B-splines, as a numerical optimization method for minimizing weight while satisfying all of the constraints.
Results: The optimum shape design of fillet in tension bars used as the numerical example in order to verify the formulation and the implementation of the proposed technique. The numerical results show our technique is efficient and precise.
Conclusion: From the research that has been performed, it is possible to conclude that the optimal shape of the top half of the fillet under stress constraint based on magneto-thermo-viscoelasticity is crucial when magneto-thermoviscoelastic field is sensitive to boundary shape. Also from this knowledge of the variation of the displacements and temperature sensitivities with time for magneto-thermo-viscoelastic FGA structures, we can design various magneto-thermoviscoelastic structures to meet specific engineering requirements and utilize within which to place new information can be more effective.

Keywords: Dual reciprocity boundary element method; Shape Optimization; Design sensitivity analysis; Implicit differentiation method; Feasibledirection method; Functionally graded anisotropic structures; Golden-section search algorithm.

2010 mathematics subject classification: 65M38 - 65K05 - 74B05 - 74E05 -74F05 - 74H05 - 74H15 - 74S20 - 90C31.

1 Introduction

Biot [1] formulated the classical coupled thermo-elasticity (CCTE) theory to overcome the paradox ingrained in the classical uncoupled thermo-elasticity (CUTE) theory that elastic changes have no effect on temperature. The parabolic type of heat equations for both theories predicting infinite speeds of propagation for heat waves which is a physically unreasonable result. Lord and Shulman [2] introduced an extended thermo-elasticity (ETE) theory, which is also known as the theory of generalized thermoelasticity with one relaxation time. The hyperbolic heat equation connected with this theory resolves the infinite speeds of propagation paradox ingrained in both the CUTE and CCTE theories of thermoelasticity. Another thermoelasticity theory that admits the second sound effect is reported by Green and Lindsay [3] who developed temperature-rate-dependent thermo-elasticity (TRDTE) theory, which is also called as the theory of generalized thermoelasticity with two relaxation times by introducing two relaxation times that relate the stress and entropy to the temperature. After that, an alternative approach in the formulation of a theory predicting the finite propagation speed of the thermal disturbances is due to Green and Naghdi [4,5] where they developed three models for generalized thermoelasticity which are labeled as models I, II and III.

In the past few decades, the scientific research in thermoelasticfunctionally graded anisotropic (FGA) structureshas become very important due to its manyengineering industries and applications [6-25]. In recent years,the structural optimization research for thermoelastic FGA structures has become a rapidly developing area of research in computational mechanics [26-28].

The dual reciprocity boundary element method (DRBEM) is a very effective method for converting the domain integral into a boundary, it has been highly successful in a very wide range of engineering applications [29-39].

Based on the approach presented in [40], the purpose of this paper is to propose a new shape optimization technique for rotating magneto-thermo-viscoelastic FGA structures placed in a constant primary magnetic field and subjected to a moving heat source in the context of the Green and Naghdi theory of type III. A predictor-corrector implicit-implicit time-stepping staggered algorithm was developed and implemented for use with the bicubic B-splines DRBEM to obtain the solution for the displacement and temperature fields. An implicit differentiation method of the dual reciprocity boundary integral equation with respect to design variables is used to calculate shape displacements and temperature sensitivities of anisotropic materials with very high accuracy. The feasible direction method based on golden-section search algorithm was used as a

numerical optimization strategy for minimizing weight while satisfying all of the constraints. The optimum shape design of the fillet in tension bars used as the numerical example in order to verify the formulation and the implementation of the proposed technique.

2 Formulation of the Problem

We shall consider the FGA structure in x_1x_2-plane occupies the region Ω under magneto-thermo-visco-mechanical effects. Also, we have assumed in this paper that the structure graded along the $0x_1$ direction.

The governing equations for rotating magneto-thermo-viscoelastic FGA structures in the context of the Green and Naghdi theory of type III can be written as (Fahmy [41])

$$\sigma_{ab,b} + \tau_{ab,b} - \rho(x+1)^m \Sigma^2 x_a = \rho(x+1)^m \ddot{u}_a, \tag{1}$$

$$\sigma_{ab} = (x+1)^m \left[C_{abfg} \aleph u_{f,g} - \beta_{ab}(T - T_0 + \tau_1 \dot{T}) \right], \tag{2}$$

$$\tau_{ab} = \mu(x+1)^m \left(\tilde{h}_a H_b + \tilde{h}_b H_a - \delta_{ba}(\tilde{h}_f H_f) \right), \tag{3}$$

$$\left[k^*_{ab} + k_{ab} \frac{\partial}{\partial \tau} \right] T_{,ab} + \rho \dot{\mathfrak{X}} = \rho c (x+1)^m \ddot{T} + \beta_{ab} T_0 \ddot{u}_{a,b} \tag{4}$$

Where σ_{ab} is the mechanical stress tensor, τ_{ab} is the Maxwell's electromagnetic stress tensor, u_f is the displacement, T is the temperature, T_0 is the reference temperature, C_{abfg} and β_{ab} are respectively, the constant elastic moduli and stress-temperature coefficients of the anisotropic medium, $\aleph = \left(1 + \mathsf{v}_0 \frac{\partial}{\partial \tau}\right)$ is the viscoelastic material constant, v_0 is the viscoelastic relaxation time, μ is the magnetic permeability, h is the perturbed magnetic field, H is the magnetic intensity vector, Σ is the uniform angular velocity, k_{ab} is the heat conductivity coefficients, k^*_{ab} is the second order tensor of new material constants associated with the Green and Naghdi theories, ρ is the density, c is the specific heat capacity, τ is the time, $\mathfrak{X}$ is the moving heat source and m is a rational number.

In addition to that, the following conditions for our problem could be considered.

$$C_{abfg} = C_{fgab} = C_{bafg}, \beta_{ab} = \beta_{ab}, (k_{12})^2 - k_{11}k_{22} < 0, \aleph = \left(1 + \mathsf{v}_0 \frac{\partial}{\partial \tau}\right)$$

A superposed dot denotes differentiation with respect to the time and a comma followed by a subscript denotes partial differentiation with respect to the corresponding coordinates.

3 Numerical Implementation

By using Eqs. (2) and (3), we can write (1) as follows

$$L_{ab}u_f = \rho \ddot{u}_a - \left(D_a T - \rho \Sigma^2 x_a\right) = f_{ab} \tag{5}$$

where the inertia term $\rho \ddot{u}_a$, the temperature gradient $D_a T$ and rotation term $\rho \Sigma^2 x_a$ are treated as the body forces.

The field equations may be expressed in operator form as follows

$$L_{gb}u_f = f_{gb} \tag{6}$$

$$L_{ab}T = f_{ab} \tag{7}$$

where the operators L_{gb}, f_{gb}, L_{ab} and f_{ab} are defined as follows:

$$L_{gb} = D_{abf}\frac{\partial}{\partial x_b} + D_{af} + \Lambda D_{a1f}, \qquad f_{gb} = \rho\ddot{u}_a\text{-}D_aT + \rho\Sigma^2 x_a \tag{8}$$

$$L_{ab} = k^*_{ab}\frac{\partial}{\partial x_a}\frac{\partial}{\partial x_b}, \qquad f_{ab} = k_{ab}\dot{T}_{,ab} + \rho c(x+1)^m\ddot{T} + \beta_{ab}T_0\ddot{u}_{a,b}\text{-}\rho\dot{\mathfrak{x}}. \tag{9}$$

where

$$D_{abf} = C_{abfg}\aleph\varepsilon, \qquad \varepsilon = \frac{\partial}{\partial x_g}, \qquad D_{af} = \mu H_0^2\left(\frac{\partial}{\partial x_a} + \delta_{a1}\Lambda\right)\frac{\partial}{\partial x_f},$$

$$D_a = \text{-}\beta_{ab}\left(\frac{\partial}{\partial x_b} + \delta_{b1}\Lambda + \tau_1\left(\frac{\partial}{\partial x_b} + \Lambda\right)\frac{\partial}{\partial\tau}\right), \ \Lambda = \frac{m}{x+1}.$$

Using the weighted residual method (WRM), the differential equation (16) can be transformed into the following integral equation

$$\int_R (L_{gb}u_f\text{-}f_{gb})u^*_{da}\,dR = 0 \tag{10}$$

Now, we choose the fundamental solution u^*_{df} defined by

$$L_{gb}u^*_{df} = \text{-}\delta_{ad}\delta(x,\xi) \tag{11}$$

as weighting function

The corresponding traction field can be written as

$$t^*_{da} = C_{abfg}\aleph u^*_{df,g}n_b \tag{12}$$

The magneto-thermo-viscoelastic traction vector can be represented by

$$t_a = \frac{\bar{t}_a}{(x+1)^m} = \left(C_{abfg}\aleph u_{f,g}\text{-}\beta_{ab}(T + \tau_1\dot{T})\right)n_b \tag{13}$$

Applying integration by parts to (10) using the sifting property of the Dirac distribution, with (12) and (13), we can write the following elastic integral representation formula

$$u_d(\xi) = \int_C \left(u^*_{da}t_a\text{-}t^*_{da}u_a + u^*_{da}\beta_{ab}Tn_b\right)dC\text{-}\int_R f_{gb}u^*_{da}dR \tag{14}$$

The fundamental solution T^* of the thermal operator L_{ab} is defined by

$$L_{ab}T^* = \text{-}\delta(x,\xi) \tag{15}$$

By implementing the WRM and integration by parts, the differential equation (7) is converted to the following thermal reciprocity equation

$$\int_R \left(L_{ab}TT^{*}\text{-}L_{ab}T^{*}T\right)dR = \int_C \left(q^{*}T\text{-}qT^{*}\right)dC \tag{16}$$

Where the heat fluxes are independent of the elastic field and can be expressed as follows:

$$q = \text{-}k_{ab}T_{,b}n_a \tag{17}$$

$$q^{*} = \text{-}k_{ab}T^{*}_{,b}n_a \tag{18}$$

By using the sifting property, we get from (16) the thermal integral representation formula

$$T(\xi) = \int_C \left(q^{*}T\text{-}qT^{*}\right)dC \text{-} \int_R f_{ab}T^{*}dR \tag{19}$$

The integral representation formulae of elastic and thermal fields (14) and (19) can be combined to form a single equation as follows

$$\begin{bmatrix} u_d(\xi) \\ T(\xi) \end{bmatrix} = \int_C \left\{ \text{-}\begin{bmatrix} t^{*}_{da} & \text{-}u^{*}_{da}\beta_{ab}n_b \\ 0 & \text{-}q^{*} \end{bmatrix}\begin{bmatrix} u_a \\ T \end{bmatrix} + \begin{bmatrix} u^{*}_{da} & 0 \\ 0 & \text{-}T^{*} \end{bmatrix}\begin{bmatrix} t_a \\ q \end{bmatrix}\right\} dC \text{-} \int_R \begin{bmatrix} u^{*}_{da} & 0 \\ 0 & \text{-}T^{*} \end{bmatrix}\begin{bmatrix} f_{gb} \\ \text{-}f_{ab} \end{bmatrix} dR \tag{20}$$

For our purpose, it is convenient to use the following contracted notation for introducing the generalized magneto-thermo-viscoelastic vectors and tensors:

$$U_A = \begin{cases} u_a & a = A = 1,2,3 \\ T & A = 4 \end{cases} \tag{21}$$

$$\mathsf{T}_A = \begin{cases} t_a & a = A = 1,2,3 \\ q & A = 4 \end{cases} \tag{22}$$

$$U^{*}_{DA} = \begin{cases} u^{*}_{da} & d = D = 1,2,3; a = A = 1,2,3 \\ 0 & d = D = 1,2,3; A = 4 \\ 0 & D = 4; a = A = 1,2,3 \\ \text{-}T^{*} & D = 4; A = 4 \end{cases} \tag{23}$$

$$\tilde{T}^{*}_{DA} = \begin{cases} t^{*}_{da} & d = D = 1,2,3; a = A = 1,2,3 \\ \text{-}\tilde{u}^{*}_{d} & d = D = 1,2,3; A = 4 \\ 0 & D = 4; a = A = 1,2,3 \\ \text{-}q^{*} & D = 4; A = 4 \end{cases} \tag{24}$$

$$\tilde{u}^{*}_{d} = u^{*}_{da}\beta_{af}n_f \tag{25}$$

Using the contracted notation described in equations (21) - (25) above, the magneto-thermo-viscoelastic representation formula (20) can be written as:

$$U_D(\xi) = \int_C \left(U^{*}_{DA}\mathsf{T}_A\text{-}\tilde{T}_{DA}U_A\right)dC \text{-} \int_R U^{*}_{DA}S_A dR \tag{26}$$

The vector S_A can be splitted as follows:

$$S_A = S_A^0 + S_A^T + S_A^{\dot{T}} + S_A^{\ddot{T}} + S_A^{\ddot{u}} \tag{27}$$

Where

$$S_A^0 = \begin{cases} \rho\Sigma^2 x_a & A = 1,2,3 \\ \rho\ddot{\mathfrak{X}} & A = 4 \end{cases} \tag{28}$$

$$S_A^T = \omega_{AF} U_F \quad \text{with} \quad \omega_{AF} = \begin{cases} -D_a & A = 1,2,3; F = 4 \\ 0 & \text{otherwise} \end{cases} \tag{29}$$

$$S_A^{\dot{T}} = \Gamma_{AF} \dot{U}_F \quad \text{with} \quad \Gamma_{AF} = \begin{cases} -k_{ab} \dfrac{\partial}{\partial x_a} \dfrac{\partial}{\partial x_b} & A = 4; F = 4 \\ 0 & \text{otherwise} \end{cases} \tag{30}$$

$$S_A^{\ddot{T}} = \delta_{AF} \ddot{U}_F \quad \text{with} \quad \delta_{AF} = \begin{cases} -c\rho(x+1)^m & A = 4; F = 4 \\ 0 & \text{otherwise} \end{cases} \tag{31}$$

$$S_A^{\ddot{u}} = \beth \ddot{U}_F \quad \text{with} \quad \beth = \begin{cases} \rho & A = 1,2,3;\ F = 1,2,3, \\ -T_0 \beta_{fg} \varepsilon & A = 4;\ F = 4 \end{cases} \tag{32}$$

The magneto-thermo-viscoelastic representation formula (20) can also be written in matrix form as follows:

$$[S_A] = \begin{bmatrix} \rho\Sigma^2 x_a \\ \rho\ddot{\mathfrak{X}} \end{bmatrix} + \begin{bmatrix} -D_a T \\ 0 \end{bmatrix} + \begin{bmatrix} 0 \\ -k_{ab}\dot{T}_{,ab} \end{bmatrix} - \rho c(x+1)^m \begin{bmatrix} 0 \\ \ddot{T} \end{bmatrix} + \begin{bmatrix} \rho\ddot{u}_a \\ -\beta_{fg} T_0 \ddot{u}_{f,g} \end{bmatrix} \tag{33}$$

Our task now is to implement the DRBEM. To transform the domain integral in (26) to the boundary, we approximate the source vector S_A in the domain as usual by a series of given tensor functions f_{AE}^q and unknown coefficients α_E^q

$$S_A \approx \sum_{q=1}^{E} f_{AE}^q \alpha_E^q \tag{34}$$

Thus, the magneto-thermo-viscoelastic representation formula (26) can be written in the following form

$$U_D(\xi) = \int_C \left(U_{DA}^* T_A - \tilde{T}_{DA}^* U_A \right) dC - \sum_{q=1}^{N} \int_R U_{DA}^* f_{AE}^q \, dR \, \alpha_E^q \tag{35}$$

By applying the WRM to the following inhomogeneous elastic and thermal equations:

$$L_{gb} u_{fe}^q = f_{ae}^q \tag{36}$$

$$L_{ab} T^q = f_{pi}^q \tag{37}$$

where the weighting functions are selected as the elastic and thermal fundamental solutions u_{da}^* and T^*. Then The elastic and thermal representation formulae are given as follows (Fahmy [41])

$$u_{de}^q(\xi) = \int_C \left(u_{da}^* t_{ae}^q - t_{da}^* u_{ae}^q \right) dC - \int_R u_{da}^* f_{ae}^q \, dR \tag{38}$$

$$T^q(\xi) = \int_C \left(q^* T^q - q^q T^*\right) dC - \int_R f^q T^* dR \tag{39}$$

By combining the dual representation formulae of elastic and thermal fields, we obtain the following combined single equation

$$U^q_{DE}(\xi) = \int_C \left(U^*_{DA} T^q_{AE} - T^*_{DA} U^q_{AE}\right) dC - \int_R U^*_{DA} f^q_{AE} dR \tag{40}$$

With the substitution of (40) into (35), the dual reciprocity representation formula of coupled magneto-thermo-viscoelasticity can be expressed as follows

$$U_D(\xi) = \int_C \left(U^*_{DA} T_A - \check{T}^*_{DA} U_A\right) dC + \sum_{q=1}^{E} \left(U^q_{DE}(\xi) + \int_C \left(T^*_{DA} U^q_{AE} - U^*_{DA} T^q_{AE}\right) dC \right) \alpha^q_E \tag{41}$$

Now the source term in equation (40) is approximated by a series of known tensor functions $\mathrm{f}^{\mathrm{q}}_{\mathrm{GE}}$ and unknown tensor coefficients $\alpha^{\mathrm{q}}_{\mathrm{E}}$ as follows

$$U^*_{DA} f^q_{AE} \approx \sum_{\mathrm{q}=1}^{\mathrm{N}} \mathrm{f}^{\mathrm{q}}_{\mathrm{GE}} \alpha^{\mathrm{q}}_{\mathrm{E}} \tag{42}$$

According to the Lyapunov-Tauber theorem, we assumed that we have bicubic B-spline surface, as follows (Ushatov et al. [42])

$$\vec{\mathrm{Q}}(\bar{\xi}, \bar{\eta}) = \sum_{\mathrm{i}=0}^{2\mathrm{M}+2} \sum_{\mathrm{j}=0}^{\mathrm{N}+3} \mathrm{V}_{\mathrm{i,j}} \mathrm{B}_{\mathrm{i,j}}(\bar{\xi}, \bar{\eta}) \tag{43}$$

where $\bar{\xi}$ and $\bar{\eta}$ are the entire surface coordinates, $\mathrm{B}_{\mathrm{i,j}}(\bar{\xi}, \bar{\eta}) = \mathrm{B}_{\mathrm{i}}(\bar{\xi})\mathrm{B}_{\mathrm{j}}(\bar{\eta})$ is a tensor-product B-spline, the functions $\mathrm{B}_{\mathrm{i}}(\xi)$ and $\mathrm{B}_{\mathrm{j}}(\eta)$ are univariate cubic B-splines and the control points $(\mathrm{x}_{1_{\mathrm{i,j}}}, \mathrm{x}_{2_{\mathrm{i,j}}}, \mathrm{x}_{3_{\mathrm{i,j}}})$ are arranged in a rectangular topology $\vec{\mathrm{V}}_{\mathrm{i,j}}$, then we have

$$U^q_{AE}(\bar{\xi}, \bar{\eta}) = \sum_{\mathrm{m}=0}^{2\mathrm{M}+2} \sum_{\mathrm{j}=0}^{\mathrm{N}+3} \mathrm{a}_{\mathrm{mj}} \mathrm{B}_{\mathrm{m}}(\xi)\, \mathrm{B}_{\mathrm{j}}(\eta) \tag{44}$$

where ξ and η are single surface patch only coordinates.

Hence, the traction particular solution $\mathrm{T}^{\mathrm{q}}_{\mathrm{AE}}$ and the source function $\mathrm{f}^{\mathrm{q}}_{\mathrm{GE}}$ can be evaluated as

$$T^q_{AE} = \mathrm{C}_{\mathrm{fGHi}} U^q_{DE,i} \mathrm{n}_{\mathrm{f}}, \quad \mathrm{L}_{\mathrm{GH}} U^q_{DE}(\xi) = \mathrm{f}^{\mathrm{q}}_{\mathrm{GE}} \tag{45}$$

According to the steps described in Fahmy [43], the dual reciprocity boundary integral equation (41) can be written in the following system of equations

$$\check{\zeta} U - \eta T = \left(\zeta \breve{U} - \eta \breve{\wp}\right) \alpha \tag{46}$$

where the matrix ζ includes the fundamental solution T^*_M and the matrix $\check{\zeta}$ includes the modified fundamental tensor $\check{T}^*_M$ with the coupling term

According to the technique proposed by Partridge et al. (Partridge et al. [32]), the generalized displacements U_F are approximated in terms of a series of known tensor functions f_{FD}^q and unknown tensor coefficients γ_D^q

$$U_F \approx \sum_{q=1}^{N} f_{FD}^q(x)\gamma_D^q \tag{47}$$

Where

$$f_{FD}^q = \begin{cases} f_{fd}^q & f = F = 1,2,3; d = D = 1,2,3 \\ f^q & F = 4; \quad D = 4 \\ 0 & \text{otherwise} \end{cases} \tag{48}$$

The generalized displacement gradients can be approximated in terms of the derivatives of tensor functions as follows

$$U_{F,g} \approx \sum_{q=1}^{N} f_{FD,g}^q(x)\gamma_K^q \tag{49}$$

Now, the source terms are approximated using Eq. (29) as follows

$$S_A^T = \sum_{q=1}^{N} S_{AF} f_{FD,g}^q \gamma_D^q \tag{50}$$

Now, we use the point collocation procedure described in Gaul et al. (Gaul et al. [44]) and applied it to (34) and (47). This leads to the following system of equations

$$\check{S} = J\alpha, \qquad U = J'\gamma \tag{51}$$

Similarly, the application of the point collocation procedure to the source terms equations (50), (30), (31) and (32) leads to the following system of equations

$$\check{S}^T = \mathscr{B}^T\gamma \tag{52}$$

$$\check{S}^{\dot{T}} = \overline{\Gamma}_{AF}\dot{U} \tag{53}$$

$$\check{S}^{\ddot{T}} = \bar{\delta}_{AF}\ddot{U} \tag{54}$$

$$\check{S}^{\ddot{u}} = \overline{\exists}\ddot{U} \tag{55}$$

where $[\Gamma_{AF}]$, $[\delta_{AF}]$ and $[\exists]$ are matrices.

Solving the system (51) for α and γ yields

$$\alpha = J^{-1}\check{S} \qquad \gamma = J'^{-1}U \tag{56}$$

Now, the coefficients α can be expressed in terms of nodal values of the unknown displacements $\breve{U}$, velocities $\dot{\breve{U}}$ and accelerations $\ddot{\breve{U}}$ as follows:

$$\alpha = J^{-1}\left(\check{S}^0 + \mathscr{B}^T J'^{-1}U + \overline{\Gamma}_{AF}\dot{U} + \left(\overline{\exists} + \bar{\delta}_{AF}\right)\ddot{U}\right) \tag{57}$$

By developing and implementing an implicit-implicit staggered algorithm of Farhat et al. (Farhat et al. [45]) for use with the DRBEM for solving the governing equations which can be written in a more convenient form after substitution of Eq. (57) into Eq. (46) as follows:

$$\tilde{\tilde{M}}\,\ddot{U} + \tilde{\tilde{\Gamma}}\,\dot{U} + \tilde{\tilde{K}}\,U = \tilde{\tilde{Q}} \tag{58}$$

$$\tilde{\tilde{X}}\,\ddot{T} + \tilde{\tilde{A}}\,\dot{T} + \tilde{\tilde{B}}\,T = \tilde{\tilde{Z}}\,\ddot{U} + \tilde{\tilde{R}} \tag{59}$$

Where

$$V = \left(\zeta \breve{U} - \eta \breve{\varphi}\right) J^{-1}, \qquad \tilde{\tilde{M}} = V\left(\bar{\bar{\jmath}} + \bar{\delta}_{AF}\right), \qquad \tilde{\tilde{\Gamma}} = V\bar{\bar{\Gamma}}_{AF},$$
$$\tilde{\tilde{K}} = -\zeta + V\breve{\mathcal{B}}^{T} J^{-1}, \qquad \tilde{\tilde{Q}} = -\eta\breve{T} + V\breve{S}^{0}, \qquad \tilde{\tilde{X}} = -\rho c (x+1)^{m},$$
$$\tilde{\tilde{A}} = k_{ab}\frac{\partial}{\partial x_a}\frac{\partial}{\partial x_b}, \qquad \tilde{\tilde{B}} = k^{*}_{ab}\frac{\partial}{\partial x_a}\frac{\partial}{\partial x_b}, \qquad \tilde{\tilde{Z}} = \beta_{ab} T_0,$$
$$\tilde{\tilde{R}} = -\rho\dot{\mathfrak{x}}$$

Where $\tilde{\tilde{A}}$, $\tilde{\tilde{B}}$, V, $\tilde{\tilde{M}}$, $\tilde{\tilde{\Gamma}}$ and $\tilde{\tilde{K}}$ represent the capacity, conductivity, volume, mass, damping and stiffness matrices, respectively, $\ddot{U}, \dot{U}, U, T$ and $\tilde{\tilde{Q}}$ represent the acceleration, velocity, displacement, temperature and external force vectors, respectively, $\tilde{\tilde{Q}}$, $\tilde{\tilde{Z}}$ and $\tilde{\tilde{R}}$ are coupling matrices.

Hence, the governing equations will take the following coupled system (Farhat et al. [45]):

$$\tilde{\tilde{M}}\,\ddot{U}_{n+1} + \tilde{\tilde{\Gamma}}\,\dot{U}_{n+1} + \tilde{\tilde{K}}\,U_{n+1} = \tilde{\tilde{Q}}^{p}_{n+1} \tag{60}$$

$$\tilde{\tilde{X}}\,\ddot{T}_{n+1} + \tilde{\tilde{A}}\,\dot{T}_{n+1} + \tilde{\tilde{B}}\,T_{n+1} = \tilde{\tilde{Z}}\,\ddot{U}_{n+1} + \tilde{\tilde{R}} \tag{61}$$

where $\tilde{\tilde{Q}}^{p}_{n+1} = -\eta T^{p}_{n+1} + V\breve{S}^{0}$ and T^{p}_{n+1} is the predicted temperature.

Integrating Eq. (58) with the use of trapezoidal rule and Eq. (60), we obtain

$$\dot{U}_{n+1} = \dot{U}_n + \frac{\Delta\tau}{2}\left(\ddot{U}_{n+1} + \ddot{U}_n\right)$$
$$= \dot{U}_n + \frac{\Delta\tau}{2}\left[\ddot{U}_n + \tilde{\tilde{M}}^{-1}\left(\tilde{\tilde{Q}}^{p}_{n+1} - \tilde{\tilde{\Gamma}}\,\dot{U}_{n+1} - \tilde{\tilde{K}}\,U_{n+1}\right)\right] \tag{62}$$

$$U_{n+1} = U_n + \frac{\Delta\tau}{2}\left(\dot{U}_{n+1} + \dot{U}_n\right)$$
$$= U_n + \Delta\tau\dot{U}_n + \frac{\Delta\tau^2}{4}\left[\ddot{U}_n + \tilde{\tilde{M}}^{-1}\left(\tilde{\tilde{Q}}^{p}_{n+1} - \tilde{\tilde{\Gamma}}\,\dot{U}_{n+1} - \tilde{\tilde{K}}\,U_{n+1}\right)\right] \tag{63}$$

From Eq. (62) we have

$$\dot{U}_{n+1} = \bar{\bar{Y}}^{-1}\left[\dot{U}_n + \frac{\Delta\tau}{2}\left[\ddot{U}_n + \tilde{\tilde{M}}^{-1}\left(\tilde{\tilde{Q}}^{p}_{n+1} - \tilde{\tilde{K}}\,U_{n+1}\right)\right]\right] \tag{64}$$

where $\bar{\bar{Y}} = \left(I + \frac{\Delta\tau}{2}\tilde{\tilde{M}}^{-1}\tilde{\tilde{\Gamma}}\right)$

Substituting from Eq. (64) into Eq. (63), we derive

$$U_{n+1} = U_n + \Delta\tau \dot{U}_n + \frac{\Delta\tau^2}{4}\left[\ddot{U}_n + \tilde{M}^{-1}\left(\tilde{\tilde{Q}}^p_{n+1} - \tilde{\tilde{\Gamma}}\tilde{\tilde{Y}}^{-1}\left[\dot{U}_n + \frac{\Delta\tau}{2}\left[\ddot{U}_n + \tilde{M}^{-1}\left(\tilde{\tilde{Q}}^p_{n+1} - \tilde{\tilde{K}}\, U_{n+1}\right)\right]\right] - \tilde{\tilde{K}}\, U_{n+1}\right)\right] \quad (65)$$

Substituting $\dot{U}^i_{n+1}$ from Eq. (64) into Eq. (60) we obtain

$$\ddot{U}_{n+1} = \tilde{M}^{-1}\left[\tilde{\tilde{Q}}^p_{n+1} - \tilde{\tilde{\Gamma}}\left[\tilde{Y}^{-1}\left[\dot{U}_n + \frac{\Delta\tau}{2}\left[\ddot{U}_n + \tilde{M}^{-1}\left(\tilde{\tilde{Q}}^p_{n+1} - \tilde{\tilde{K}}\, U_{n+1}\right)\right]\right] - \tilde{\tilde{K}}\, U_{n+1}\right]\right] \quad (66)$$

Integrating the heat equation (59) using the trapezoidal rule, and Eq. (61) we get

$$\dot{T}_{n+1} = \dot{T}_n + \frac{\Delta\tau}{2}\left(\ddot{T}_{n+1} + \ddot{T}_n\right) = \dot{T}_n + \frac{\Delta\tau}{2}\left(\tilde{\tilde{X}}^{-1}\left[\tilde{\tilde{\mathbb{Z}}}\,\ddot{U}_{n+1} + \tilde{\tilde{\mathbb{R}}} - \tilde{\tilde{A}}\,\dot{T}_{n+1} - \tilde{\tilde{B}}\, T_{n+1}\right] + \ddot{T}_n\right) \quad (67)$$

$$T_n + \frac{\Delta\tau}{2}\left(\dot{T}_{n+1} + \dot{T}_n\right) = T_n + \Delta\tau\dot{T}_n + \frac{\Delta\tau^2}{4}\left(\ddot{T}_n + \tilde{\tilde{X}}^{-1}\left[\tilde{\tilde{\mathbb{Z}}}\,\ddot{U}_{n+1} + \tilde{\tilde{\mathbb{R}}} - \tilde{\tilde{A}}\,\dot{T}_{n+1} - \tilde{\tilde{B}}\, T_{n+1}\right]\right) \quad (68)$$

From Eq. (67) we get

$$\dot{T}_{n+1} = Y^{-1}\left[\dot{T}_n + \frac{\Delta\tau}{2}\left(\tilde{\tilde{X}}^{-1}\left[\tilde{\tilde{\mathbb{Z}}}\,\ddot{U}_{n+1} + \tilde{\tilde{\mathbb{R}}} - \tilde{\tilde{B}}\, T_{n+1}\right] + \ddot{T}_n\right)\right] \quad (69)$$

where $Y = \left(I + \frac{1}{2}\tilde{\tilde{A}}\Delta\tau\tilde{\tilde{X}}^{-1}\right)$

Substituting from Eq. (69) into Eq. (68), we have

$$T_{n+1} = T_n + \Delta\tau\dot{T}_n + \frac{\Delta\tau^2}{4}\left(\ddot{T}_n + \tilde{\tilde{X}}^{-1}\left[\tilde{\tilde{\mathbb{Z}}}\,\ddot{U}_{n+1} + \tilde{\tilde{\mathbb{R}}} - \tilde{\tilde{A}}\left(Y^{-1}\left[\dot{T}_n + \frac{\Delta\tau}{2}\left(\tilde{\tilde{X}}^{-1}\left[\tilde{\tilde{\mathbb{Z}}}\,\ddot{U}_{n+1} + \tilde{\tilde{\mathbb{R}}} - \tilde{\tilde{B}}\, T_{n+1}\right] + \ddot{T}_n\right)\right]\right) - \tilde{\tilde{B}}\, T_{n+1}\right]\right) \quad (70)$$

Substituting $\dot{T}^i_{n+1}$ from Eq. (69) into Eq. (61) we obtain

$$\ddot{T}_{n+1} = \tilde{\tilde{X}}^{-1}\left[\tilde{\tilde{\mathbb{Z}}}\,\ddot{U}_{n+1} + \tilde{\tilde{\mathbb{R}}} - \tilde{\tilde{A}}\left(Y^{-1}\left[\dot{T}_n + \frac{\Delta\tau}{2}\left(\tilde{\tilde{X}}^{-1}\left[\tilde{\tilde{\mathbb{Z}}}\,\ddot{U}_{n+1} + \tilde{\tilde{\mathbb{R}}} - \tilde{\tilde{B}}\, T_{n+1}\right] + \ddot{T}_n\right)\right]\right) - \tilde{\tilde{B}}\, T_{n+1}\right] \quad (71)$$

Now, our proposed predictor-corrector procedure for the solution of (65) and (70) is as follows (Fahmy [46-48]):

(1) Predict the displacement field: $U^p_{n+1} = U_n$
(2) Substituting for $\dot{U}_{n+1}$ and $\ddot{U}_{n+1}$ from equations (62) and (60) respectively in Eq. (70) and
(3) Solve the resulted equation for the temperature field
(4) Correct the displacement field using the computed temperature field for the Eq. (65)

(5) Compute $\dot{U}_{n+1}$, $\ddot{U}_{n+1}$, $\dot{T}_{n+1}$ and $\ddot{T}_{n+1}$ from Eqs. (64), (66), (67) and (71) respectively.

4 Shape Design Sensitivity and Optimization

Thus, the design sensitivity analysis is performed by implicit differentiation of equation (60) for the displacements and implicit differentiation of equation (61) for temperature that describes the structural response with respect to the design variables $\mathrm{x_h}$ which are the coordinates of several nodes on the movable part of the boundary. After obtaining the displacement gradients, the stress gradients can be obtained.

let R be a closed bounded plane region whose boundary Γ consisting of a finite number of smooth curves and assuming that m and w are continuous functions and have continuous partial derivatives with respect to x_1 and x_2.

$$\iint_R \left(\frac{\partial w}{\partial x_1} - \frac{\partial m}{\partial x_2}\right) dx_1 dx_2 = \int_\Gamma (m\, dx_1 + w\, dx_2) \tag{72}$$

By using the Green's theorem, the area $\bar{A}$ of the domain $\Omega\left(\bar{A} = \iint_R dx_1 dx_2\right)$ can be written in terms of a line integral over the boundary

$$\bar{A} = \frac{1}{2}\int_\Gamma (x_1\, dx_2 - x_2\, dx_1) \tag{73}$$

If the boundary of the structure is discretized into Qquadratic isoparametric boundary elements, and the coordinates at nodal points can be expressed as

$$x_m(\xi) = N^c(\xi) x_m^c \tag{74}$$

where $N^c(\xi)$ quadratic shape function corresponding to the cth quadrilateral element's node number, and ξ is the intrinsic coordinate for the element. Therefore, the area of the domain can be calculated as follows

$$\bar{A} = \frac{1}{2}\sum_{b=1}^{Q}\int_{-1}^{1} [x_1(\xi) n_1 + x_2(\xi) n_2]\, J(\xi) d\xi \tag{75}$$

$J(\xi)$ is the Jacobian matrix of the transformation and $n_1$andn_2 are direction cosines of the unit normal vector to the surface of the structure which may be written as

$$n_1 = \frac{dx_2}{d\bar{A}} = \frac{dx_2/d\xi}{d\bar{A}/d\xi} = \frac{dx_2/d\xi}{J(\xi)} \tag{76}$$

$$n_2 = -\frac{dx_1}{d\bar{A}} = -\frac{dx_1/d\xi}{d\bar{A}/d\xi} = -\frac{dx_1/d\xi}{J(\xi)} \tag{77}$$

Substitution of equations (76) and (77) into equation (75) yields

$$\bar{A} = \frac{1}{2}\sum_{b=1}^{Q}\int_{-1}^{1}\left[x_1(\xi)\frac{dx_2}{d\xi} - x_2(\xi)\frac{dx_1}{d\xi}\right]d\xi \tag{78}$$

The weight derivative can be calculated by differentiating (75) with respect to the design variable based on the consideration that, if $x_\hbar$ is the x_1 coordinate of a movable node, then

$$\frac{\partial}{\partial x_\hbar}\left(\frac{dx_2(\xi)}{d\xi}\right) = 0 \tag{79}$$

and

$$\frac{\partial}{\partial x_\hbar}\left(x_2(\xi)\right) = 0 \tag{80}$$

Therefore

$$\frac{\partial \bar{A}}{\partial x_\hbar} = \frac{1}{2}\sum_{b=1}^{Q}\int_{-1}^{1}\left[\frac{\partial x_1(\xi)}{\partial x_\hbar}\frac{dx_2}{d\xi} - x_2(\xi)\frac{\partial}{\partial x_\hbar}\left(\frac{dx_1}{d\xi}\right)\right]d\xi \tag{81}$$

If $x_\hbar$ is the x_2 coordinate of a movable node, then

$$\frac{\partial}{\partial x_\hbar}\left(\frac{dx_1(\xi)}{d\xi}\right) = 0 \tag{82}$$

and

$$\frac{\partial}{\partial x_\hbar}\left(x_1(\xi)\right) = 0 \tag{83}$$

Therefore

$$\frac{\partial \bar{A}}{\partial x_\hbar} = \frac{1}{2}\sum_{b=1}^{Q}\int_{-1}^{1}\left[x_1(\xi)\frac{\partial}{\partial x_\hbar}\left(\frac{dx_2}{d\xi}\right) - \frac{\partial x_2(\xi)}{\partial x_\hbar}\left(\frac{dx_1}{d\xi}\right)\right]d\xi \tag{84}$$

where weight minimization is equivalent to area minimization.

The general problem that we discuss in the present paper is the minimization of structural weight which must satisfy constraints on stresses and geometry. Since both stress and weight constraints are non-linear functions of the design variables, then the feasible direction approach has been employed as the computational optimization technique. This method determines a usable-feasible direction where the design point can be moved in the design space.

Assuming the weight as the objective function that we want to

Minimize $\bar{A}(x_\hbar)$ (85)

Subject to

$$\chi_m(x_\hbar) \le \mathsf{Y}_\mathfrak{m}, \quad \mathfrak{m} = 1, \dots, M \tag{86}$$

$$\mathcal{D}_j(x_\hbar) = \Sigma_j, \quad j = 1, \dots, N \tag{87}$$

$$x_\hbar^\omega \le x_\hbar \le x_\hbar^\varpi \tag{88}$$

where $x_\hbar = [x_1, x_2, \dots, x_L]^T$, $x_\hbar^\omega$ and $x_\hbar^\varpi$ are upper and lower limits of the designvariables respectively, and R is the domain occupied by the structure.

To solve the current general shape optimization problem, both the objective function and the constraints are nonlinear functions of the design variables. It is very difficult to solve the set of nonlinear equations (85)-(88) analytically, so numerical feasible direction method that starts with the current initial design x_0, then update using following iteration process until we obtain the optimum design:

$$x_{\hbar+1} = x_\hbar + s_\hbar d_\hbar \tag{89}$$

where h is the iteration number, the line step parameter $s_\hbar$ determines the amount of change in x to find the minimum design point along the search direction $d_\hbar$.

The iteration process is repeated until convergence of the error function, i.e.

$$\bar{A}(x_{\hbar+1})\text{-}\bar{A}(x_\hbar) \le \varepsilon \tag{90}$$

which can be defined as

$$d_\hbar = \text{-}H^\hbar \nabla \bar{A}(x_\hbar) \tag{91}$$

where $H^\hbar$ is the $\hbar$-th approximation of the inverse Hessian matrix, which can be given by

$$H^{\hbar+1} = \left[I - \frac{P^\hbar Q^\hbar}{(P^\hbar)^T Q^\hbar}\right] H^\hbar \left[I - \frac{Q^\hbar (P^\hbar)^T}{(P^\hbar)^T Q^\hbar}\right] + \frac{P^\hbar (Q^\hbar)^T}{(P^\hbar)^T Q^\hbar} \tag{92}$$

where $\boldsymbol{I}$ denote the identity matrix and $(\,)^T$ denote the transpose of the matrix

$$P^\hbar = x_{\hbar+1} \text{-} x_\hbar \tag{93}$$

and

$$Q^\hbar = \nabla \bar{A}(x_{\hbar+1}) \text{-} \nabla \bar{A}(x_\hbar) \tag{94}$$

$$H^0 = I \tag{95}$$

5 Numerical Results and Discussion

We assume that moving heat source takes the following form (Fahmy [49])

$$\mathfrak{X} = \frac{\mathfrak{X}_0 H(\upsilon\tau)\sinh(x_1)}{\sqrt{x_2^2 + \upsilon^2}} \tag{96}$$

Where H, υ and $\mathfrak{X}_0$ are respectively the Heaviside unit step function, heat source velocity and heat source strength.

The optimum shape design of the fillet in tension bars used as the numerical example in order to verify the formulation and the implementation of the proposed technique presented in this paper, the material chosen for the fillet is monoclinic graphite-epoxy material is chosen for the purpose of numerical calculations, the physical data for which is given as follows (Fahmy [50]):

Elasticity tensor

$$C_{abfg} = \begin{bmatrix} 430.1 & 130.4 & 18.2 & 0 & 0 & 201.3 \\ 130.4 & 116.7 & 21.0 & 0 & 0 & 70.1 \\ 18.2 & 21.0 & 73.6 & 0 & 0 & 2.4 \\ 0 & 0 & 0 & 19.8 & -8.0 & 0 \\ 0 & 0 & 0 & -8.0 & 29.1 & 0 \\ 201.3 & 70.1 & 2.4 & 0 & 0 & 147.3 \end{bmatrix} \text{GPa} \tag{97}$$

Mechanical temperature coefficient

$$\beta_{ab} = \begin{bmatrix} 1.01 & 2.00 & 0 \\ 2.00 & 1.48 & 0 \\ 0 & 0 & 7.52 \end{bmatrix} \cdot 10^6 \ \ \text{N/ Km}^2 \tag{98}$$

Tensor of thermal conductivity is

$$k_{ab} = \begin{bmatrix} 5.2 & 0 & 0 \\ 0 & 7.6 & 0 \\ 0 & 0 & 38.3 \end{bmatrix} \text{W/km} \tag{99}$$

Mass density $\rho = 7820$ kg/ m^3 and heat capacity $c = 461$ J/(kg K), $H_0 = 1000000$ Oersted, $\mu = 0.5$ Gauss/Oersted, $\aleph = 2$, $\hbar = 2$, $\Delta\tau = 0.0001$, $T_0 = 1$.

The present work should be applicable to any magneto-thermo-visco-elastic shape optimization problem in a rotating FGA structure. The example considered by Li et al. [51] may be considered as a special case of the current general problem.

In the special case under consideration.According to the symmetry, only the top half of the fillet is considered (Lee and Kwak [52]). The elements, dimensions, mechanical and thermal boundary conditions of the fillet are shown in Fig. 1.

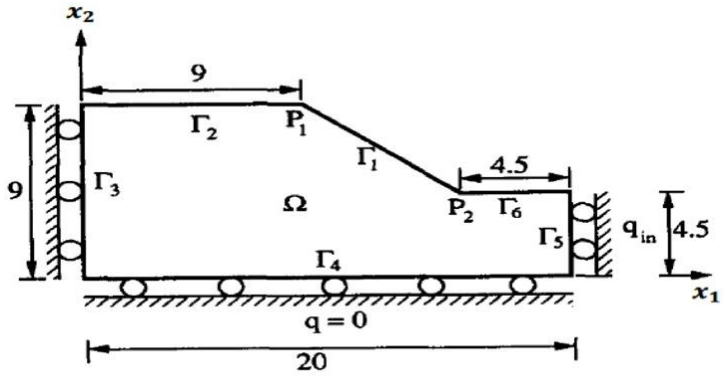

Fig. 1. Mechanical and thermal boundary conditions of a fillet.

The segment Γ_4 is the centerline segment of the fillet. The considered model has been discretized using 33 quadratic elements to describe the optimization problem which is mathematically translated into determining the best shape of Γ_1 which is to be varied to minimize use of the material and met all stress requirements

and the initial shape design chosen as a straight line between fixed points P_1 and P_2, also, the shape design variables are selected and numbered from 1 to 9, and small boundary Γ_k is specified at each quadratic element on Γ_1 for generating 10 constraints. as shown in Fig. 2.

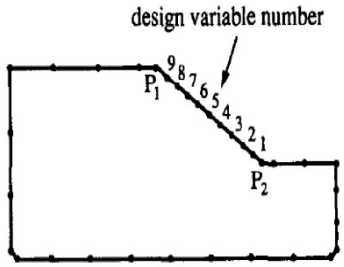

Fig. 2. Dual reciprocity boundary element model for initial shape design of the fillet.

At the optimum process, the acceptable violation of each constraint is within 10% of its allowable value, and the values of stress constraints at the initial and optimum design are listed in Table 1 with the notice that (10% corresponds to E-01 in Table 1).

Table 1. Stress constraints values at the initial and optimum design when $q_{in} = 1800\ W/m^2$

Constraint numer	Initial	Optimum
1	4.5482E-01	-1.2331E-01
2	-9.1304E-02	-1.5253E-05
3	-2.5581E-01	6.9390E-07
4	-3.6572E-01	-1.3360E-06
5	-4.5381E-01	3.2370E-06
6	-5.3212E-01	1.8790E-05
7	-6.0711E-01	-2.5555E-04
8	-6.8462E-01	-1.3490E-02
9	-7.7191E-01	-8.8070E-01
10	-8.9253E-01	-9.7520E-01

The optimum shapes of the deterministic design are obtained for different values of q_{in}: 1500, 1600, 1700 and 1800 W/m^2. Sensitivities are computed when $q_{in} = 1800\ W/m^2$ as seen in Fig. 3.

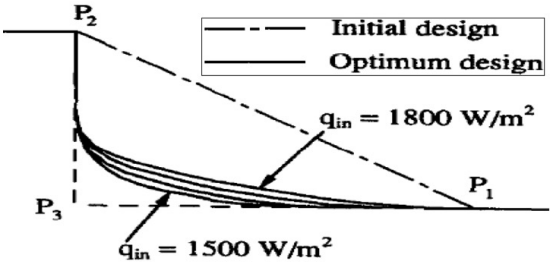

Fig. 3. Optimum shapes of the fillet.

The displacement sensitivities variations with the time τ are plotted in Figs. 4 and 5 and the temperature sensitivity variation with the time τ is plotted in Fig. 6 to verify the formulation and the implementation of the DRBEM technique.

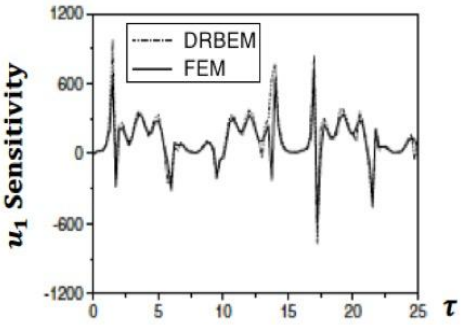

Fig. 4. Variation of the displacement u_1 Sensitivity with time τ.

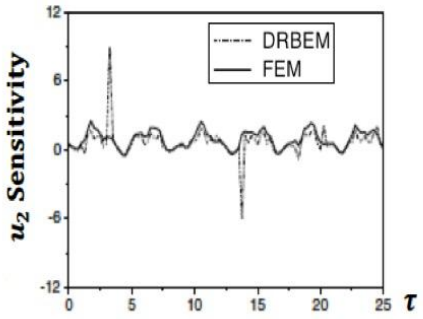

Fig. 5. Variation of the displacement u_2 Sensitivity with time τ.

It is shown from these figures that the DRBEM results are in excellent agreement with those obtained using the finite element method (FEM) of Li et al. (Li et al. [51]). Our results thus confirm that our technique is efficient and precise.

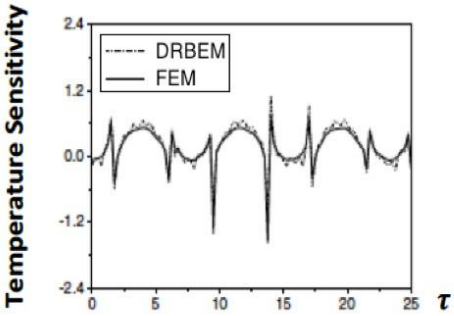

Fig. 6. Variation of the temperature Sensitivity with time τ.

It is noted that the BEM results obtained with a relative coarse discretization (32 elements) are still more accurate than the FEM results which are based on 7264 elements. As a result of the small number of elements in the BEM case the required computing power is much smaller than in the FEM case (see Table 2).

Table 2. Comparison of computer resources needed for FEM and DRBEM modelling of the top half of the fillet

	FEM	DRBEM
Number of nodes	22239	33
Number of elements	7264	32
CPU-Time [min.]	120	2
Memory [Mbyte]	100	0.5
Disc space [Mbyte]	200	0
Accuracy of results [%]	2.7	1.7

The proposed technique in the present paper should be applicable to any shape optimization problem of generalized magneto-thermoviscoelastic anisotropic material.

6 Conclusion

The dual reciprocity boundary element method is more easy, efficient and cost effective computational technique which provides an excellent alternative to the prevailing finite element method for the solution of a wide range of scientific and engineering problems and it is widely used by mathematicians and engineers for this purpose, it only needs to solve the unknowns on the boundaries, the results of all variables at any point in the considered problem are more precise because the integration operation of DRBEM is smoother than differentiation operation FEM.

For open or closed boundary problem, the users of DRBEM need only to deal with real boundaries. Most magneto-thermoviscoelasticoptimization problems are associated with open boundary problems. For these open boundary problems, the users of FEM use artificial boundaries, which are difficult to deal with numerically. So, DRBEM becomes the best method for magneto-thermoviscoelastic optimization problems.

Also, from the results of the current paper, it is possible to conclude that the optimal shape of the top half of the fillet under stress constraint based on magneto-thermo-viscoelasticity is crucial when magneto-thermo-viscoelastic field is sensitive to boundary shape. Also from this knowledge of the displacements and temperature sensitivitiesvariation of the with time for rotating magneto-thermoviscoelastic FGA structures, we can design various optimalrotating magneto-thermoviscoelastic structures to meet specific engineering requirements and understand the key engineering decisions.

As the future work,the dual reciprocity method, which is used in the present paper can be developed and used to solve non-linear and time-dependent complex engineering and physical problems. The method can be applied to define sources over the whole domain or only on part of it.

Competing Interests

Author has declared that no competing interests exist.

References

[1] Biot M. Thermoelasticity and irreversible thermo-dynamics. J. Appl. Phys. 1956;27:249-253.

[2] Lord HW, Shulman Y. A generalized dynamical theory of thermoelasticity. J. Mech. Phys. Solids 1967;15:299-309.

[3] Green AE, Lindsay KA. Thermoelasticity. J. Elast. 1972;2:1-7.

[4] Green AE, Naghdi PM. On undamped heat waves in an elastic solid. J. Therm. Stresses. 1992;15:252-264.

[5] Green AE, Naghdi PM. Thermoelasticity without energy dissipation. J. Elast. 1993;31:189-208.

[6] Oden JT, Armstrong WH. Analysis of nonlinear, dynamic coupled thermoviscoelasticity problems by the finite element method. Comput. Struct. 1971;1:603-621.

[7] Misra SC, Samanta SC, Chakrabarti AK. Transient magnetothermoelastic waves in a viscoelastic half-space produced by ramp-type heating of its surface. Comput. Struct. 1992;43:951-957.

[8[El-Naggar AM, Abd-Alla AM, Fahmy MA and Ahmed SM. Thermal stresses in a rotating non-homogeneous orthotropic hollow cylinder. Heat Mass Transfer. 2002;39:41-46.

[9] El-Naggar AM, Abd-Alla AM, Fahmy MA. The propagation of thermal stresses in an infinite elastic slab. Appl. Math. Comput. 2004;157:307-312.

[10] Abd-Alla AM, El-Naggar AM, Fahmy MA. Magneto-thermoelastic problem in non-homogeneous isotropic cylinder. Heat Mass Transfer. 2003;39:625-629.

[11] Abd-Alla AM, Fahmy MA, El-Shahat TM. Magneto-thermo-elastic problem of a rotating non-homogeneous anisotropic solid cylinder. Arch. Appl. Mech. 2008;78:135-148.

[12] Fahmy MA. Thermoelastic stresses in a rotating non-homogeneous anisotropic body. Numerical Heat Transfer. Part A. 2008;53:1001-1011.

[13] Fahmy MA. Finite difference algorithm for transient magneto-thermo-elastic stresses in a non-homogeneous solid cylinder. Int. J. Mater. Eng. Technol. 2010;3:87-93.

[14] Fahmy MA. Transient magneto-thermo-viscoelastic stresses in a rotating nonhomogeneous anisotropic solid with and without a moving heat source. J. Eng. Phys. Thermophys. 2012;85:950-958.

[15] Fahmy MA, El-Shahat TM. The effect of initial stress and inhomogeneity on the thermoelastic stresses in a rotating anisotropic solid. Arch. Appl. Mech. 2008;78:431-442.

[16] Shariyat M, Lavasani SMH, Khaghani M. Nonlinear transient thermal stress and elastic wave propagation analyses of thick temperature-dependent FGM cylinders, using a second-order point-collocation method. Appl. Math. Modell. 2010;34:898-918.

[17] Kumar AV, Parthasarathy A. Topology optimization using B-spline finite elements. Struct. Multidisc. Optim. 2011;44: 471.

[18] Bobaru F, Mukherjee S. Meshless approach to shape optimization of linear thermoelastic solids. International Journal for Numerical Methods in Engineering. 2002;53:765-796

[19] Rangelov T, Stoynov Y, Dineva P. Dynamic fracture behavior of functionally graded magnetoelectroelastic solids by BIEM. Int. J. Solids Struct. 2011;48:2987-2999.

[20] Arani AG, Kolahchi R, Barzoki AAM, Loghman A. Electro-thermo-mechanical behaviors of FGPM spheres using analytical method and ANSYS software. Appl. Math. Modell. 2012;36:139-157.

[21] Zhang W, Yang J, Xu Y, Gao T. Topology optimization of thermoelastic structures: Mean compliance minimization or elastic strain energy minimization, Struct. Multidisc. Optim. 2014;49:417–429.

[22] Gutiérrez S,Mura J.Shape optimization for a seepage problem with low contrast core. Appl. Math. Modell. 2016;40:1825-1835.

[23] Singh P, Couckuyt I, Elsayed K, Deschrijver D, Dhaene T. Shape optimization of a cyclone separator using multi-objective surrogate-based optimization. Appl. Math. Modell. 2016;40:4248-4259.

[24] Casas WJP, Pavanello R. Optimization of fluid-structure systems by eigenvalues gap separation with sensitivity analysis. Appl. Math. Modell. 2017;42:269-289.

[25] Hussein OS, Mulani SB. Multi-dimensional optimization of functionally graded material composition using polynomial expansion of the volume fraction. Struct. Multidisc. Optim. 2017;56:271-284.

[26] Erman Z, Fenner RT. Three-dimensional design optimization using the boundary integral equation method. J. Strain Anal. 1996;31:289-298.

[27] Faure A, Michailidis G, Parry G, Vermaak N, Estevez R. Design of thermoelastic multi-material structures with graded interfaces using topology optimization, Structural and Multidisciplinary Optimization. 2017;56:823–837.

[28] Fahmy MA. Shape design sensitivity and optimization of anisotropic functionally graded smart structures using bicubic B-splines DRBEM. Engineering Analysis with Boundary Elements. 2018;87:27-35.

[29] Nardini D, Brebbia CA. A new approach to free vibration analysis using boundary elements, in: C.A. Brebbia (Ed.), Boundary elements in engineering, Springer, Berlin. 1982;312-326.

[30] Brebbia CA, Telles JCF, Wrobel L. Boundary element techniques in engineering. Springer-Verlag, New York, 1984.

[31] Wrobel LC, Brebbia CA. The dual reciprocity boundary element formulation for nonlinear diffusion problems. Comput. Methods Appl. Mech. Eng. 1987;65:147-164.

[32] Partridge PW, Brebbia CA, Wrobel LC. The dual reciprocity boundary element method, Computational Mechanics Publications, Southampton; 1992.

[33] Partridge PW, Wrobel LC.The dual reciprocity boundary element method for spontaneous ignition. Int. J. Numer. Methods Eng. 1990;30:953–963.

[34] Partridge PW, Brebbia CA. Computer implementation of the BEM dual reciprocity method for the solution of general field equations. Commun. Appl. Numer. Math. 1990;6:83-92.

[35] Fahmy MA. A time-stepping DRBEM for magneto-thermo-viscoelastic interactions in a rotating nonhomogeneous anisotropic solid. Int. J. Appl. Mech. 2011;3:1-24.

[36] Fahmy MA. Numerical modeling of transient magneto-thermo-viscoelastic waves in a rotating nonhomogeneous anisotropic solid under initial stress. Int. J. Model. Simul. Sci. Comput. 2012;3:125002.

[37] Fahmy MA. Transient magneto-thermo-elastic stresses in an anisotropic viscoelastic solid with and without moving heat source. Numer. Heat Transfer, Part A. 2012;61:547-564.

[38] Fahmy MA. The effect of rotation and inhomogeneity on the transient magneto-thermoviscoelastic stresses in an anisotropic solid. ASME J. Appl. Mech. 2012;79:1015.

[39] Fahmy MA. Computerized boundary element solutions for thermoelastic problems: Applications to functionally graded anisotropic structures, LAP Lambert Academic Publishing, Saarbrücken, Germany; 2017.

[40] Fahmy MA. Implicit–explicit time integration DRBEM for generalized magneto-thermoelasticity problems of rotating anisotropic viscoelastic functionally graded solids. Eng. Anal. Boundary Elem. 2013;37:107-115.

[41] Fahmy MA. Generalized magneto-thermo-viscoelastic problems of rotating functionally graded anisotropic plates by the dual reciprocity boundary element method. J. Therm. Stresses. 2013;36:1-20.

[42] Ushatov R, Power H, Rêgo Silva JJ. Uniform bicubic B-splines applied to boundary element formulation for 3-D scalar problems, Engineering Analysis with Boundary Elements. 1994;13:371-381.

[43] Fahmy MA. A time-stepping DRBEM for the transient magneto-thermo-visco-elastic stresses in a rotating non-homogeneous anisotropic solid. Eng. Anal. Boundary Elem. 2012;36:335-345.

[44] Gaul L, Kögl M, Wagner M. Boundary element methods for engineers and scientists. Springer-Verlag, Berlin; 2003.

[45] Farhat C, Park KC, Dubois-Pelerin Y. An unconditionally stable staggered algorithm for transient finite element analysis of coupled thermoelastic problems. Comput. Methods Appl. Mech. Eng. 1991;85:349-365.

[46] Fahmy MA. A three-dimensional generalized magneto-thermo viscoelastic problem of a rotating functionally graded anisotropic solids with and without energy dissipation. Numer. Heat Transfer, Part A. 2013;63:713-733.

[47] Fahmy MA. A time-stepping DRBEM for 3D anisotropic functionally graded piezoelectric structures under the influence of gravitational waves. In: Rodrigues H., Elnashai A., Calvi G. (eds) Facing the Challenges in Structural Engineering. GeoMEast 2017. Sustainable Civil Infrastructures. Springer, Cham. 2018;350-365.

[48] Fahmy MA. A computerized DRBEM model for generalized magneto-thermo-visco-elastic stress waves in functionally graded anisotropic thin film/substrate structures. Lat. Am. J. Solids Struct. 2014;11:369-385.

[49] Fahmy MA. Transient magneto-thermoviscoelastic plane waves in a non-homogeneous anisotropic thick strip subjected to a moving heat source. Appl. Math. Modell. 2012;36:4565-4578.

[50] Fahmy MA. Shape design sensitivity and optimization for two-temperature generalized magneto-thermoelastic problems using time-domain DRBEM, Journal of Thermal Stresses. 2018;41:119-138

[51] Li L, Zhang G, Khandelwal K. Topology optimization of structures with gradient elastic material. Struct. Multidisc. Optim. 2017;56:371–390.

[52] Lee BY, Kwak BM. Shape optimization of two-dimensional thermoelastic structures using boundary integral equation formulation. Comput. Struct. 1991;2017;41:709-722.

Peer-review history:
The peer review history for this paper can be accessed here (Please copy paste the total link in your browser address bar)
http://sciencedomain.org/review-history/22562